Biogeosciences, 10, 3593–3604, 2013
www.biogeosciences.net/10/3593/2013/
doi:10.5194/bg-10-3593-2013

Biogeosciences Open Access

Impact of CO_2 and climate on Last Glacial maximum vegetation – a factor separation

M. Claussen[1], K. Selent[1,2,*], V. Brovkin[1], T. Raddatz[1], and V. Gayler[1]

[1]Max Planck Institute for Meteorology, Hamburg, Germany
[2]Meteorological Institute, University of Hamburg, Germany
[*]now at: Deutsches Klimarechenzentrum DKRZ, Hamburg, Germany

Correspondence to: M. Claussen (martin.claussen@zmaw.de)

Received: 5 October 2012 – Published in Biogeosciences Discuss.: 12 November 2012
Revised: 12 April 2013 – Accepted: 29 April 2013 – Published: 3 June 2013

Abstract. The factor separation of Stein and Alpert (1993) is applied to simulations with the MPI Earth system model to determine the factors which cause the differences between vegetation patterns in glacial and pre-industrial climate. The factors firstly include differences in the climate, caused by a strong increase in ice masses and the radiative effect of lower greenhouse gas concentrations; secondly, differences in the ecophysiological effect of lower glacial atmospheric CO_2 concentrations; and thirdly, the synergy between the pure climate effect and the pure effect of changing physiologically available CO_2. It is has been shown that the synergy can be interpreted as a measure of the sensitivity of ecophysiological CO_2 effect to climate. The pure climate effect mainly leads to a contraction or a shift in vegetation patterns when comparing simulated glacial and pre-industrial vegetation patterns. Raingreen shrubs benefit from the colder and drier climate. The pure ecophysiological effect of CO_2 appears to be stronger than the pure climate effect for many plant functional types – in line with previous simulations. The pure ecophysiological effect of lower CO_2 mainly yields a reduction in fractional coverage, a thinning of vegetation and a strong reduction in net primary production. The synergy appears to be as strong as each of the pure contributions locally, but weak on global average for most plant functional types. For tropical evergreen trees, however, the synergy is strong on global average. It diminishes the difference between glacial and pre-industrial coverage of tropical evergreen trees, due to the pure climate effect and the pure ecophysiological CO_2 effect, by approximately 50 per cent.

1 Introduction

During the Last Glacial Maximum some 21 000 yr ago, large parts of North America and Northern Europe were covered by ice masses, and the atmospheric concentration of greenhouse gases was lower than today. Global glacial climate was considerably colder and drier, and global vegetation patterns were different from those today. Tropical forests were presumably reduced in their extent (Crowley, 1995) with tropical rainforest being replaced by tropical seasonal forest in tropical lowlands and by xerophytic woods in tropical highlands (Elenga et al., 2000) or by savannah and tropical grassland, mainly in Latin and South America (Marchant et al., 2009). Boreal and temperate forests regressed equatorwards with a compression and fragmentation of the forest zones (Prentice et al., 2000; Tarasov et al., 2000) covering a much smaller fraction than today.

Differences between glacial and present-day potential vegetation were diagnosed by vegetation models with input from climate models (e.g. Claussen and Esch, 1994; Kutzbach et al., 1998) or by coupled climate–vegetation models where vegetation was assumed to be a function of climate in terms of moisture, temperature and insolation (e.g., Kubatzki and Claussen, 1998; Jahn et al., 2005; Roche et al., 2007). Numerous coupled and uncoupled simulations (Levis and Foley, 1999; Harrison and Prentice, 2003; Crucifix et al., 2005; Prentice et al., 2011; Woillez et al., 2011) highlighted the role of ecophysiological effects of differences in atmospheric CO_2 concentration. In an atmosphere with reduced CO_2, photorespiration increases so that net productivity is reduced. As a second indirect effect, plants increase their stomatal

conductance and their number of stomata, thereby affecting their transpiration and water-use efficiency. Subsequently, not only the dispersion of plants changes, but also the ratio between C3 and C4 plants shifts. Simulations of glacial vegetation, which take changes in the climate and the ecophysiological CO_2 effect into account, draw the same qualitatively similar picture: a strong reduction of forests in mid- and high northern latitudes was attributed to the colder climate and the presence of ice sheets where the ecophysiological effect adds to this reduction. In the tropics, the ecophysiological effect of low CO_2 appears to be the dominant factor. Globally, a shift to more open vegetation with enhanced fraction of grass coverage under reduced CO_2 is seen in the models and, consistently, a strong reduction in simulated global net primary production.

So far, few modelling studies have analyzed the relative contribution of the climate and ecophysiological effects of CO_2 to differences between glacial and present-day potential vegetation (e.g. Harrison and Prentice, 2003; Crucifix et al., 2005; Prentice et al., 2011). Little attention has been paid to the synergy between climate and ecophysiological CO_2 effect. Woillez et al. (2011) were the first to provide a set of four simulations from which the contributions due to climate, the ecophysiological effects of CO_2 and the synergy can be computed. Furthermore, they mention that the strength of the ecophysiological effect depends on the climate state, but they do not quantify this effect. In this study, the problem is reassessed by presenting a rigorous factor separation according to Stein and Alpert (1993). The factor separation is then applied to results of a global dynamic vegetation model, JSBACH, coupled to the atmospheric general circulation model ECHAM6. The resulting factors and synergies are compared with values computed from simulations by Woillez et al. (2011).

2 Methods

2.1 Factor separation

To isolate the impacts of the climate's ecophysiological CO_2 effect and synergy (when both factors are operating) on the difference between glacial and pre-industrial potential vegetation pattern, we apply the factor separation proposed by Stein and Alpert (1993). According to this method, 2^n simulations have to be provided, where n is the number of factors to be considered, which affect the result of the simulation in question. Hence for this study with $n = 2$, four simulations were set up: CTRL and CTRL-R refer to pre-industrial climate, where for CTRL-R the physiologically available CO_2 was set at glacial level of 185 ppm (the suffix R stands for reduced CO_2). Simulations LGM and LGM-E refer to glacial climate, where for LGM-E, the physiologically effective CO_2 was set at pre-industrial level of 280 ppm (the suffix E stands for enhanced CO_2). This setup is similar to the experimental design used by Woillez et al. (2011). Woillez et al. (2011) however used atmospheric CO_2 concentrations of 310 ppm, a value representative for industrial, non-equilibrium climate of the 20th century.

According to the factor separation of Stein and Alpert (1993), the pure contribution f_C due to differences in climate (including differences in ice sheet and land–sea distribution) and pure contribution f_E because of ecophysiological CO_2 effects, are given for each PFT by

$$f_C = A(\text{LGM-E}) - A(\text{CTRL}) \tag{1a}$$

$$f_E = A(\text{CTRL-R}) - A(\text{CTRL}), \tag{1b}$$

where A is the areal coverage by the PFT under consideration.

The synergy f_{CE} between factors f_C and f_E is given by:

$$\begin{aligned} f_{CE} &= A(\text{LGM}) - A(\text{CTRL}) - f_C - f_E \\ &= A(\text{LGM}) - A(\text{LGM-E}) - A(\text{CTRL-R}) \\ &\quad + A(\text{CTRL}). \end{aligned} \tag{1c}$$

Please note that the factors differ, if not the pre-industrial climate, but the climate of the Last Glacial Maximum is used as reference state, in other words

$$g_C = A(\text{CTRL-R}) - A(\text{LGM}) \tag{2a}$$

$$g_E = A(\text{LGM-E}) - A(\text{LGM}). \tag{2b}$$

f_C, f_E and g_C, g_E describe qualitatively the same processes, but only from two different perspectives. Hence there is no qualitatively new information to be gained by separately investigating f_C, f_E and g_C, g_E. Hence only factors f_C, f_E are discussed in the following.

The synergy viewed from the Last Glacial Maximum as reference state reads

$$\begin{aligned} g_{CE} &= A(\text{CTRL}) - A(\text{LGM}) - g_C - g_E \\ &= A(\text{CTRL}) - A(\text{LGM-E}) - A(\text{CTRL-R}) \\ &\quad + A(\text{LGM}). \end{aligned} \tag{2c}$$

Hence, the synergy is the same, i.e., $g_{CE} = f_{CE}$, regardless of whether the simulation CRTL or the simulation LGM is used as reference state.

How can the synergy be interpreted? By rearranging Eq. (1c) (or Eq. 2c) it becomes obvious that f_{CE} can be read as the difference between the ecophysiological effect of enhanced CO_2 in warm climate and in cold climate, in other words

$$\begin{aligned} f_{CE} &= A(\text{CTRL}) - A(\text{CTRL-R}) - (A(\text{LGM-E}) \\ &\quad - A(\text{LGM})). \end{aligned} \tag{3a}$$

Hence f_{CE} is the sensitivity of ecophysiological CO_2 effect to climate, where climate is defined in the wider sense, including changes in atmospheric conditions, ice masses and sea level.

Table 1. Boundary conditions and forcing used in the simulations referred to as CTRL, CTRL-R, LGM-E, LGM in this study. Ice sheet, topography and coastline are taken from Peltier (2004), orbital parameters from Berger (1978). These conditions are chosen according to the PMIP-2 protocol (Braconnot et al., 2007).

		CTRL	CTRL-R	LGM-E	LGM
Ice sheets, topography, coastline		Modern		ICE-G5	
Trace gases	Physiologically effective CO_2	280 ppm	185 ppm	280 ppm	185 ppm
	Radiative effective CO_2	280 ppm		185 ppm	
	CH_4 (ppbv)	760 ppb		350 ppb	
	N_2O	270 ppb		200 ppb	
Insolation	Solar constant	1365 ($W m^{-2}$)			
	Eccentricity	0.016724		0.018994	
	Obliquity	23.446°		22.949°	
	Angular precession	102.04°		114.42°	

An alternative, and equally valid, interpretation can be derived by re-arranging Eq. (3a):

$$f_{CE} = A(\text{CTRL}) - A(\text{LGM-E}) - (A(\text{CTRL-R}) - A(\text{LGM}))\,. \quad (3b)$$

This is the difference between the pure climate effect on vegetation changes under high and low physiologically effective CO_2. Hence it follows from the symmetry of Eqs. (3a) and (3b) that f_{CE} can also be interpreted as sensitivity of the pure climate effect on ecophysiologically available CO_2.

2.2 Models and model setup

This study focusses on atmosphere–vegetation interaction with prescribed atmospheric CO_2 concentrations. Hence only the terrestrial carbon pools and fluxes are allowed to vary. Sea surface temperature and sea ice conditions are prescribed from separate simulations for pre-industrial and glacial climate, respectively. This implies that feedbacks between vegetation dynamics and ocean dynamics on glacial–interglacial climate dynamics are assumed to be much smaller than atmosphere–vegetation and atmosphere–ocean feedbacks. Whether this assumption is valid has to be tested. In the case of mid-Holocene climate, this assumption seems to be valid for the model used here (Otto et al., 2009; Dallmeyer et al., 2010).

In this study, the MPI-ESM, the Earth system model developed at the Max Planck Institute for Meteorology in Hamburg, is used with the atmospheric model ECHAM6 (Stevens et al., 2013) and the land surface model JSBACH (Raddatz et al., 2007; Brovkin et al., 2009, 2013; Reick et al., 2013). The JSBACH model simulates fluxes of energy, water, momentum, and CO_2 between land and atmosphere. The modelling concept is based on a fractional structure of the land surface. Each land grid cell is divided into fractions covered with eight plant functional types (PFTs), i.e., tropical evergreen trees, tropical deciduous trees, extratropical evergreen trees, extratropical deciduous trees, raingreen shrubs, deciduous shrubs, C3 grasses, C4 grasses, and two types of bare surface (seasonally bare soil and permanently bare ground, i.e. deserts). Fractions which are excluded from vegetation dynamics (anthropogenic land cover, inland water, crops, etc.) are not taken into account in this study. The C3 and C4 photosynthetic pathway for autotrophic respiration and photosynthesis processes are based on the model by Farquhar et al. (1980) for C3 plants and Collatz et al. (1992) for C4 plants. Besides leaf phenology and photosynthetic pathway, the PFTs differ in photosynthetic capacity (Kattge et al., 2009), specific leaf area, and carbon allocation.

The version of JSBACH used here does not consider nitrogen limitation in plant growth. The simulated vegetation dynamics are based on the assumption that competition between different PFTs is determined by their relative competitiveness expressed in annual net primary productivity (NPP), bioclimatic limits, as well as natural and disturbance-driven mortality (Brovkin et al., 2009; Reick et al., 2013). Land surface albedo is mostly determined by the resulting vegetation distribution as PFTs differ in the reflectance of their canopy and whether snow on the ground is masked by the canopy (trees) or not (all other PFTs). Details of the albedo scheme are given in the appendix of Otto et al. (2011).

The sea surface temperatures for pre-industrial climate and glacial climate were prescribed by using results of earlier simulations with the ECHAM-5–MPI-OM model system at T31 resolution for the atmosphere, while the oceanic model MPI-OM (Jungclaus et al., 2006) was run at approximately 3° resolution with 40 vertical layers. The atmosphere–ocean simulations, which were initialized with boundary conditions defined within the Paleoclimate Modeling Intercomparison Project-2 (PMIP-2; Bracconot et al., 2007), were run some 2000 years to reach equilibrium (Mikolajewicz, personal communication, 2012; the model system is described in Mikolajewicz et al., 2007). Glacial ice sheet topography and coastlines are specified according to Peltier (2004) and

orbital parameters, according to Berger (1978). In the model the total land area (including ice sheets) amounts to some $142.99 \times 10^6\,km^2$ in pre-industrial and $155.15 \times 10^6\,km^2$ in LGM climate. The area covered by ice sheets increase from $14.54 \times 10^6\,km^2$ in pre-industrial to $36.61 \times 10^6\,km^2$ in LGM climate. The boundary conditions and forcing for the simulations undertaken in this study are summarized in Table 1.

Simulations were run at T31 (i.e., approximately $3.8° \times 3.8°$) resolution with 19 vertical levels. The model simulated 300 years to reach equilibrium between atmospheric and vegetation dynamics. For the first 200 yr of the simulation, vegetation dynamics were accelerated by a factor of 3. The results shown in this study have been taken from the last 100 yr of the simulation with synchronous coupling of atmospheric and vegetation dynamics.

3 Simulation results

3.1 Pre-industrial vegetation

Figure 1a, b shows the fractional coverage of each grid cell with woody vegetation (i.e., tree, shrubs) as estimated by Brovkin et al. (2009) and based on satellite data by Hansen et al. (2007) for present-day climate, as computed from the MPI-ESM simulation for pre-industrial climate (simulation CTRL). For comparison with observations, the natural tree/shrub cover simulated by the model was reduced following the reconstruction of present-day anthropogenic land cover change by Pongratz et al. (2008). The comparison of simulated woody coverage with the vegetation continuous fields by Hansen et al. (2007) was chosen, because the land-surface model JSBACH, like the model ORCHIDEE used by Woillez et al. (2011), uses the vegetation continuous field approach. Furthermore, because most above-ground carbon is stored in woody types, woody coverage is considered a decisive validation variable. Since extratropical and tropical tree PFTs do not overlap geographically, and since the fractional coverage by shrub PFTs is small, Fig. 1a, b provide a good overview of the model performance with respect to tropical and extratropical woody cover, respectively.

Comparison of the observed and simulated woody coverage reveals that the main patterns are well reproduced. The model tends to overestimate woody cover partly due to climate biases of the atmosphere model in Africa and partly due to a tendency of the vegetation model to simulate tree encroachment in dry regions (central Asia, Australia) where, according to Brovkin et al. (2009), the disturbances are underestimated in the model. The model underestimates woody coverage in Alaska and, to some degree, at high northern latitudes. There, disturbance of vegetation due to wind break is presumably too large. (For details see Brovkin et al., 2009, 2013.)

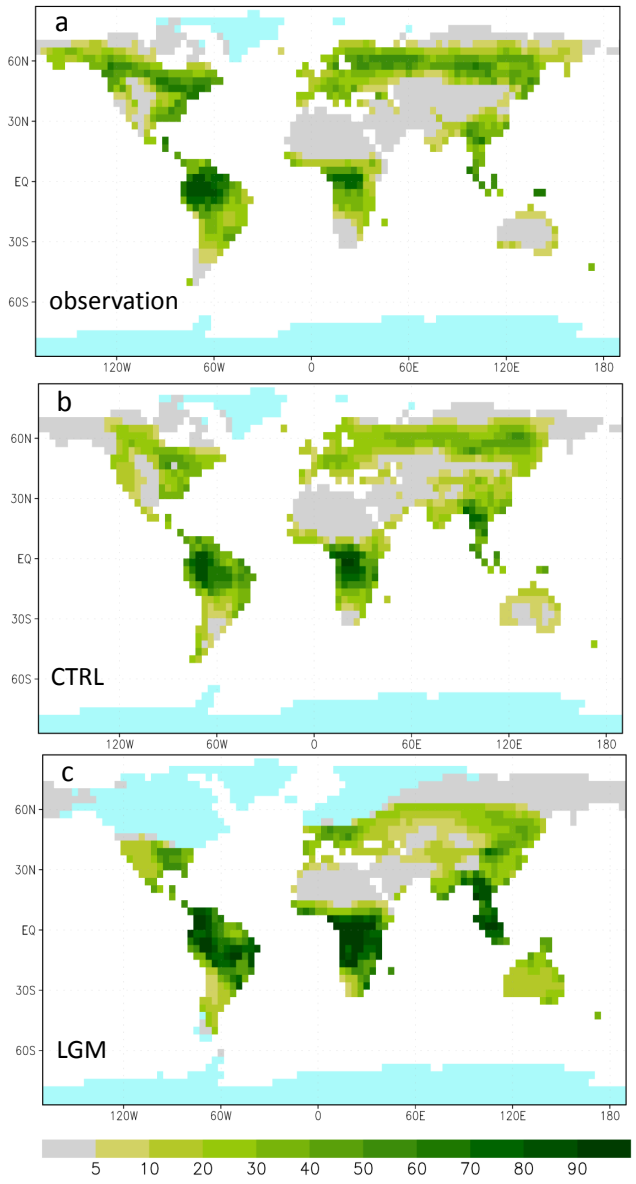

Fig. 1. (a) Present-day tree and shrub cover based on MODIS data by Hansen et al. (2007) averaged on the MPI-ESM grid (Figure taken from Brovkin et al., 2009). **(b)** Simulated tree and shrub cover in the control simulation CTRL (modified to account for historical deforestation). **(c)** Simulated tree and shrub cover in the LGM simulation.

3.2 Glacial temperature and precipitation

The MPI-ESM simulates a near-surface (2 m) air temperature for pre-industrial climate of 13.7 °C on global average and 8.2 °C on average over land. Simulated global mean precipitation is 2.78 mm/d. These values are in good agreement with recent estimates of near-surface land temperature of some 8 °C in the 19th century and 8.9 °C in the 20th entury (Rohde et al., 2013) and estimates of present-day precipitation of 2.62–2.78 mm d^{-1} (Hantel, 2005).

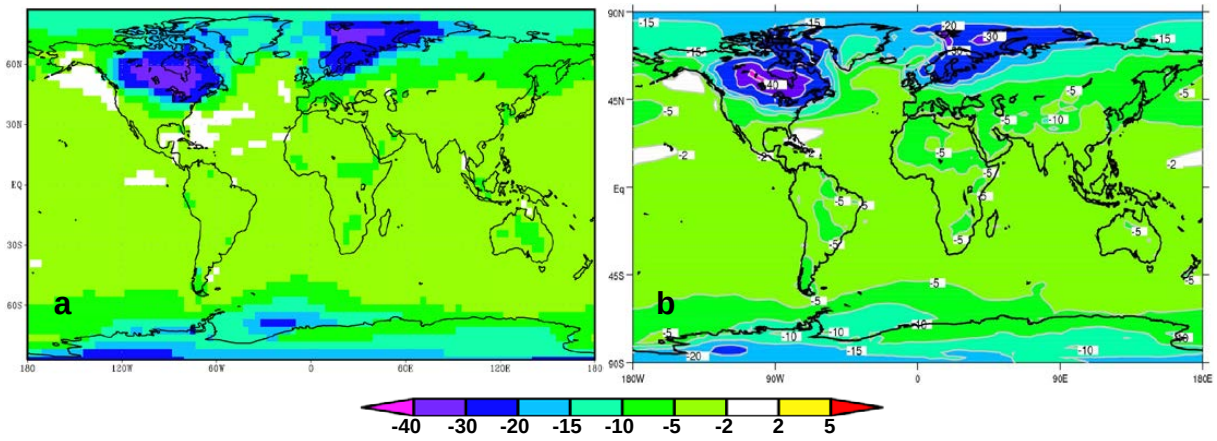

Fig. 2. Differences in annual mean 2 m air temperature (in K) between simulations of the climate of the Last Glacial Maximum and of pre-industrial climate. **(a)** Difference between the LGM and the CTL simulation, **(b)** difference of the ensemble mean of the atmosphere-ocean-vegetation model simulations of PMIP-2 (Braconnot et al., 2007); **(b)** is taken from http://pmip2.lsce.ipsl.fr

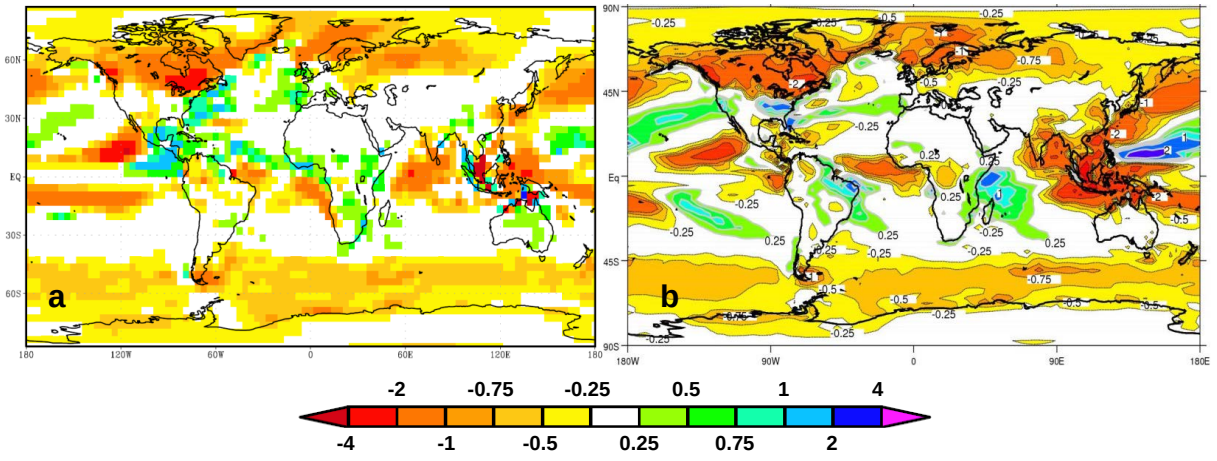

Fig. 3. Same as Fig. 2, except for differences in annual mean precipitation (in mm d^{-1}).

For the Last Glacial Maximum, the MPI-ESM yields 8.6 °C and 2.49 mm d^{-1} for global mean near-surface air temperature and precipitation, respectively. A glacial cooling of 5.1 °C and a reduction of global precipitation by some 10 % is in good agreement with the range of results of other simulations in the Paleoclimate Modeling Intercomparison Project (PMIP) (Braconnot et al., 2007). Moreover, the pattern of differences between glacial and pre-industrial climate simulated by MPI-ESM agrees with the pattern reported by PMIP (see Fig. 2a, b and Fig. 3a, b). Noteworthy exceptions include tropical Africa, where the MPI-ESM simulates a moderate increase in precipitation for LGM climate, whereas the ensemble mean of the PMIP-2 reveals some decrease.

3.3 Glacial vegetation

Figure 1c depicts the global area covered by woody PFTs in glacial climate, and Fig. 4 specifies the differences in global area covered by all PFTs between glacial and pre-industrial climate, i.e., between the simulations LGM and CTRL. In line with previous simulations, the MPI-ESM yields a decrease in areas of tropical trees (by some 20 %) and of extratropical trees (by some 45 %). The desert area increases by 36 %. The area covered by grassland decreases by some 40 %, while the area covered by shrubs increases by approximately 57 %.

A detailed comparison between simulated glacial and pre-industrial vegetation (see also Selent, 2012) shows that the northern and the southern margin of tropical evergreen trees is shifted towards the Equator (Fig. 5a). The fractional coverage of tropical evergreen trees in the inner tropics increases, including the area of the Indonesian shelf, which can be occupied by vegetation due to lower sea level during the Last Glacial Maximum. Tropical deciduous trees are reduced almost everywhere (Fig. 5b). Extratropical evergreen and deciduous trees (Fig. 5c, d) are regressed southward, and extratropical evergreen trees replace extratropical deciduous trees

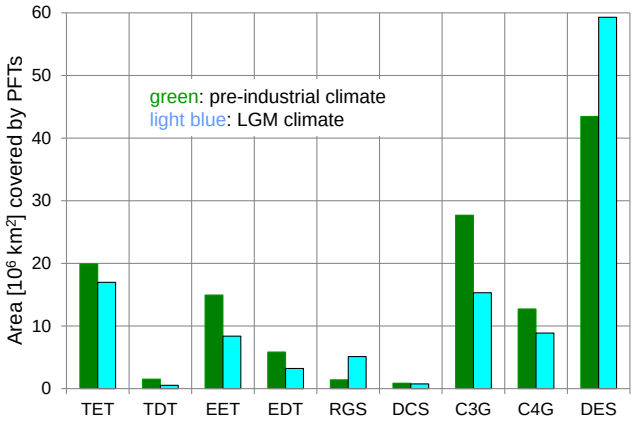

Fig. 4. Area (in $10^6\,km^2$) covered by different PFTs and bare ground for pre-industrial climate (dark green columns) and glacial climate (blue columns). The PFTs are tropical evergreen trees (TET), tropical deciduous trees (TDT), extratropical evergreen trees (EET), extratropical deciduous trees (EDT), raingreen shrubs (RGS), deciduous shrubs (DCS), C3 grass (C3G), C4 grass (C4G), and bare ground (DES).

in large parts of Europe. In turn, extratropical deciduous trees replace extratropical evergreen trees in Siberia around 60°N. Interestingly, extratropical evergreen trees and, to a much smaller extent extratropical deciduous trees, move into the tropics and outweigh tropical trees in some regions. Raingreen shrubs (Fig. 5e) are more widespread in the glacial tropics and are found in areas which in pre-industrial climate are covered by tropical trees. Hence, raingreen (or tropical and subtropical) shrubs benefit from the glacial climate in the MPI-ESM. Deciduous shrubs (Fig. 5f) are shifted southward over Eurasia, and are nearly extinct in North America, but the sum of all areas covered by deciduous shrubs remains nearly the same in glacial and pre-industrial climate. Grassland generally decreases. C3 grass (Fig. 5g) is pushed southward by the ice masses. On average, C3 grassland is reduced in all northern continents, although it is still the dominant PFT in the western part of North America, northern Siberia, and the southern part of South America (not shown). It is increased in the southern tropics. C4 grass (Fig. 5h) is reduced in almost all areas.

A detailed comparison of these results with reconstruction and previous simulations of glacial vegetation can be found in Selent (2012). In summary, the MPI-ESM captures many aspects of glacial vegetation patterns, such as the regression of forests in high northern latitudes and the expansion of bare ground found in reconstructions by Prentice et al. (2000), Tarasov et al. (2000) and Bigelow et al. (2003) and simulations by Claussen and Esch (1994), Harrison and Prentice (2003), Kutzbach et al. (1998), Levis and Foley (1999), Roche et al. (2007), and Woillez et al. (2011). The small decrease of tropical evergreen forest in the MPI-ESM agrees with the results by Woillez et al. (2011). However, in contrast to the latter study, the MPI-ESM simulates an increase in tropical evergreen forest in the inner tropics. This seems to be at variance with reconstructions by Crowley (1995) and Marchant et al. (2009). Presumably, this difference can partly be attributed to the green bias of the MPI-ESM in these regions and the moderate increase in glacial precipitation over tropical Africa, which is not found in the ensemble mean of the PMIP-2 simulations. The expansion of grasses in the tropics and extratropics, found by Levis and Foley (1999), Harrison and Prentice (2003), Crucifix et al. (2005), and Woillez et al. (2011), is missing in the MPI-ESM. However, in the MPI-ESM, C3 grass is still the dominant PFT in Siberia and southern part of South America in glacial climate where trees prevail in pre-industrial climate. Likewise, the ratio between C4 and C3 grasses increases, which is in qualitative agreement with Crucifix et al. (2005).

Regarding NPP, the MPI-ESM simulates a decrease from some $57.9\,Gt\,C\,yr^{-1}$ of NPP in pre-industrial climate to some $31.2\,Gt\,C\,yr^{-1}$ in glacial climate. These values agree well with results by Crucifix et al. (2005) of $57.5\,Gt\,C\,yr^{-1}$ and $36.6\,Gt\,C\,yr^{-1}$, for pre-industrial and glacial climate, respectively.

3.4 Factors and synergies

The pure contribution of climate, i.e., the factor f_C (Eq. 1a), including the difference in area available for vegetation growth, results in a reduction of the areal coverage of all PFT, except for raingreen shrubs (Fig. 6). In addition, the pure contribution in climate leads to a shift of vegetation pattern. This is valid for most PFTs in most regions. As an example, differences in tropical evergreen trees (TET) are presented in Fig. 7. Tropical evergreen trees are reduced at their northern and southern margins. This reduction, which can be attributed to the bioclimatic temperature limits of TET, is partly compensated by an increase in fractional coverage in the inner tropics, including an expansion of trees onto newly available land due to lower sea level. The pure contribution of climate effects favors the existence of C3 grasses at the expense of C4 grasses in most subtropical areas.

The pure contribution due to the ecophysiological effect of lower CO_2, given by the factor f_E (Eq. 1b), reduces the areal coverage of almost all PFTs (Fig. 6). Noteworthy exceptions are tropical deciduous trees (TDT) that seem to benefit from lower CO_2 (in some regions in Africa north of the Equator and in Australia, not shown). This could be caused, however, by the retreat of tropical evergreen trees in these regions. Also C4 grass benefits from a reduction in atmospheric CO_2 concentration on average over all areas covered by C4 grass. In many tropical areas, however, coverage by C4 grass decreases which is a consequence of the fact that in JSBACH, trees are always the dominant PFT in comparison with grass, i.e., grass coverage can increase only in areas where tree coverage is reduced.

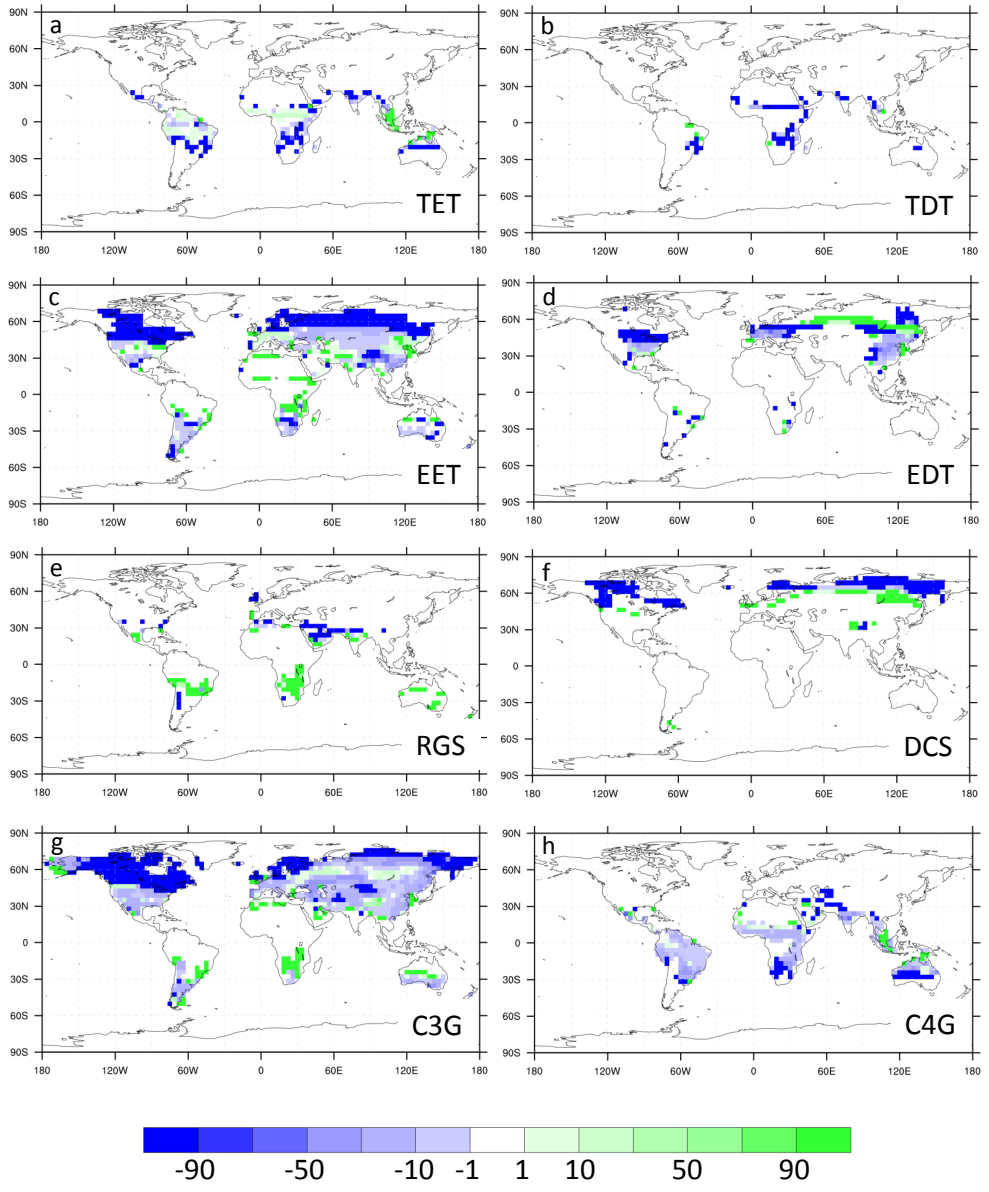

Fig. 5. Differences in fractional coverage (given in % coverage of each grid cell) between glacial and pre-industrial vegetation patterns (LGM–pre-industrial) for each PFT (for acronyms see Fig. 4).

The ecophysiological CO_2 effect leads to a strong reduction in NPP (Fig. 8). Not only the pattern, but also the difference between pre-industrial and glacial global NPP are very similar in the CTRL-R and the LGM simulations. Globally, NPP reaches some 57.9 Gt C yr^{-1} in the CTRL simulation, 32.0 Gt C yr^{-1} in the CRTL-R simulation, 55.5 Gt C yr^{-1} in the LGM-E simulation and 31.2 Gt C yr^{-1} in the LGM simulation. Consistently, the carbon stored in terrestrial biosphere is reduced between pre-industrial and glacial climate (not shown), and this is mainly caused by the ecophysiological CO_2 effect. Hence, even if there is some increase in the fractional coverage by tropical trees in South America (Fig. 5a), for example, the glacial tropical forest appears to be thinner or more open.

The synergy between the pure contribution from the climate and the ecophysiological CO_2 effect, f_{CE} (Eq. 1c), is small for most PFTs on a global scale. Figure 6 shows that the synergy between the climate and the ecophysiological CO_2 effect is considerably smaller than at least one of the pure contributions. A globally weak synergy does not imply that the synergy is weak locally. In most cases (not shown), the synergy can be as strong as the pure contributions at grid scale. Tropical evergreen trees stand out against the other PFTs as, on global average, their synergy is largest. Figure 7c reveals that the synergy is positive not everywhere,

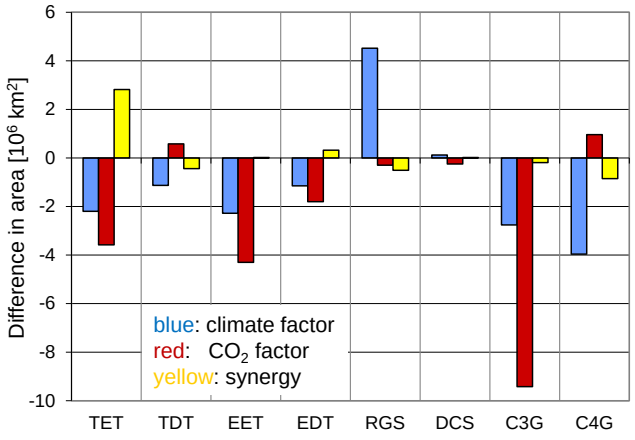

Fig. 6. Differences in global areal coverage (in 10^6 km^2) for different PFTs (for acronyms see Fig. 4). Blue columns refer to the pure contribution of differences in climate, including differences in ice sheet and land-sea distribution, to differences between glacial and pre-industrial potential coverage by each PFT (Eq. 1a). Brown columns refer to the pure contribution due to the ecophysiological effect of different CO_2 concentration in glacial and pre-industrial climate (Eq. 1b). Yellow columns depict the synergy between the pure contributions (Eq. 1c).

but positive values dominate. The synergy is larger than the pure contribution of the climate by some 30 per cent and it is reaches approximately 80 per cent of the pure ecophysiological CO_2 effect. According to the discussion in Sect. 2.1, a positive synergy means that the ecophysiological CO_2 effect is stronger in warm climate than in cold climate. Hence it is this sensitivity of the ecophysiological CO_2 to climate effect that diminishes the sum of the pure factors by some 50 per cent.

What does the synergy cause? To a large extent, synergy for tropical evergreen trees (Fig. 7c) occurs in regions where no differences in the spatial pattern of other PFTs (Fig. 5) can be found. Obviously, competition between PFTs can hardly be the main source of synergy; rather synergy is linked to the physiology of each PFT. In the Farquhar model, net primary production is a nonlinear function of temperature and CO_2, which indicates that the ecophysiological CO_2 effect on net primary production depends on temperature and vice versa, the temperature effect on net primary production is a function of ecophysiologically available CO_2. In fact, Prentice et al. (2011) and Woillez et al. (2011) already mention that the ecophysiological CO_2 effect on the distribution of vegetation varies with climate. Our study corroborates that for tropical evergreen trees, f_{CE} is positive, i.e., the ecophysiological effect of enhanced CO_2 is stronger in warm than in cold climate. For C4 grass, however, the opposite conclusion can be drawn. In this case, the synergy is negative; hence the ecophysiological effect of enhanced CO_2 decreases with warmer climate.

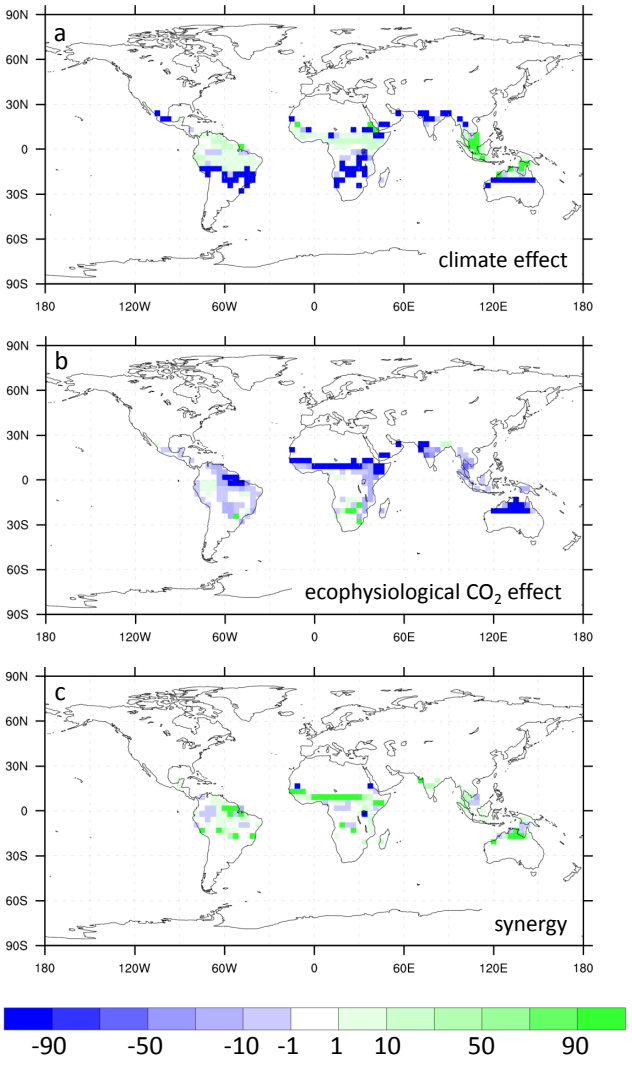

Fig. 7. Differences between glacial and pre-industrial vegetation patterns in terms of fractional coverage by tropical evergreen trees. **(a)** Differences due to the pure climatic effect, i.e., difference between simulations LGM-E and CTRL; **(b)** differences due to the pure ecophysiological CO2 effect, i.e., differences between simulations CTRL-R and CTRL; and **(c)** differences due to the synergy between climatic and ecophysiological effects, i.e., sum of simulations LGM–LGM/E–CTRL-R + CTRL.

How do these results compare with the simulations by Woillez et al. (2011)? A direct comparison is difficult because Woillez et al. (2011) use different PFTs than in this study. They differentiate between tropical, temperate and boreal trees, and they do not assign a PFT for shrubs. Hence their simulation regarding the expansion of grasses in tropics is presumably not directly comparable with the MPI-ESM simulations, which reveal a shift from trees to shrubs in this region. To facilitate some comparison, we combine tropical evergreen and deciduous trees and raingreen shrub to tropical woody plants, extratropical evergreen and decidu-

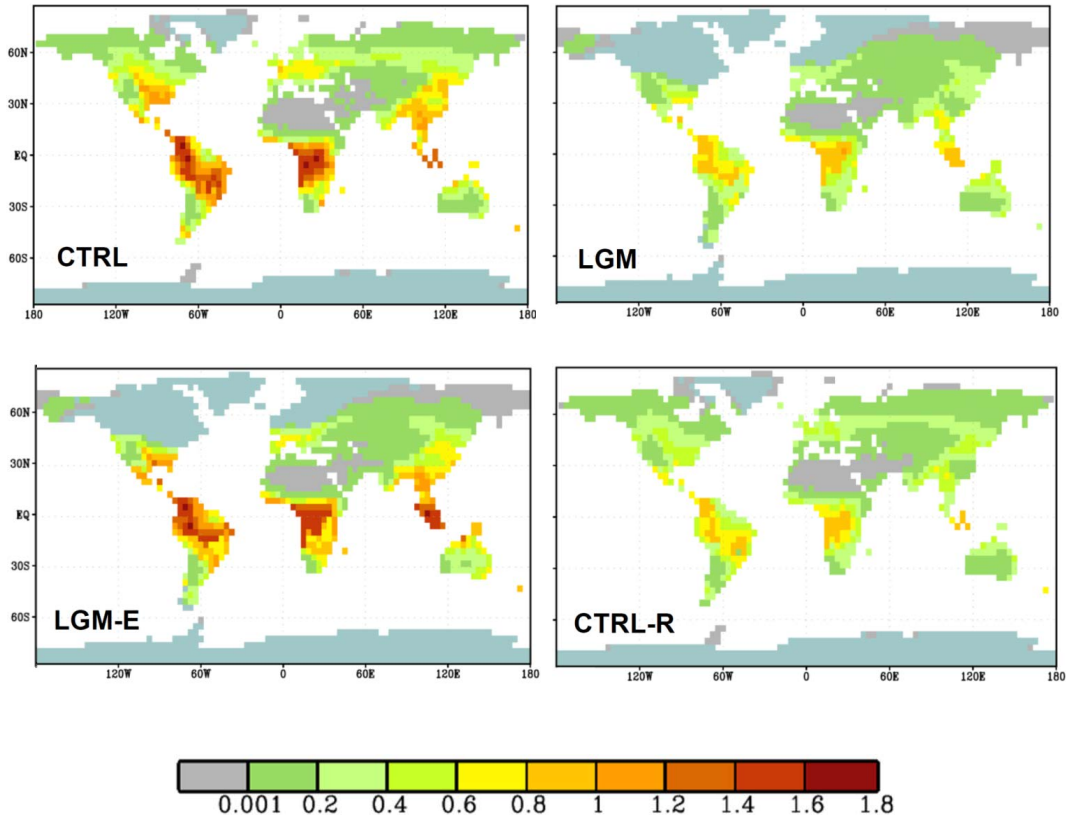

Fig. 8. Net primary production (NPP) (in $kg\,m^{-2}\,yr^{-1}$) for different simulations of pre-industrial climate (CRTL), climate of the Last Glacial Maximum (LGM), climate of the Last Glacial Maximum, but with physiologically effective CO_2 of 280 ppm as in pre-industrial climate (LGM-E), and pre-industrial climate, but with physiologically effective CO_2 of 185 ppm as in glacial climate (CTRL-R).

ous trees and deciduous shrubs to extratropical woody plant, and C3 and C4 grasses to grasses. The PFTs in the study by Woillez et al. (2011) are summed up to tropical trees, extratropical trees (comprising temperate and boreal trees) and grasses. Another complication arises from different approaches to calculate fractions of PFTs and desert (bare soil) in the models. For example, the desert fraction in JSBACH depends on the leaf area indexes of PFTs. Low glacial CO_2 concentration leads to reduced NPP for all PFTs, and therefore, to decreased vegetation area and increased desert fraction. Furthermore, we compare global areal coverage and global foliage projective coverage which are not the same variables. The foliage projective cover used by ORCHIDEE to determine the PFT fractions is based on a weighted function of canopy of PFT individuals, and sensitivity of the foliage projective cover to the changed climate and CO_2 concentration in glacial climate is different from the approach used in JSBACH. Finally, Woillez et al. (2011) used values of atmospheric CO_2 concentration of 310 ppm and 185 ppm for present-day and glacial climate, respectively. Hence the range of CO_2 changes is roughly 30 % larger than the range used in the present study, and stronger CO_2 effects – radiative and ecophysiological effects – can be expected. Hence any comparison is of qualitative nature only.

Figure 9 reveals similarities and discrepancies between the simulations by Woillez et al. (2011) and the present study. Factors and synergy of tropical woody plants agree qualitatively. The pure climate effect tends to increase the fractional coverage by tropical woody plants – in this study due to the strong increase in shrubs. The pure ecophysiological effect causes a strong decrease. The synergy is positive. The fractional coverage of extratropical woody plants decreases. The strong reduction in extratropical trees due to the pure climate effect in the simulation by Woillez et al. (2011) is not recaptured in this study. The climatically induced reduction is attributed to a strong reduction in boreal, rather than temperate, trees which could be a consequence of the strong positive bias in present-day boreal tree coverage in the model of Woillez et al. (2011). Only if high northern latitudes are extensively covered by trees in interglacial climate, the expansion of ice masses in high northern latitudes can cause large differences in boreal tree coverage. Factors and synergy of grass coverage strongly differ between studies. All factors, including synergy, indicate an increase in grass coverage in the study by Woillez et al. (2011), while the climate

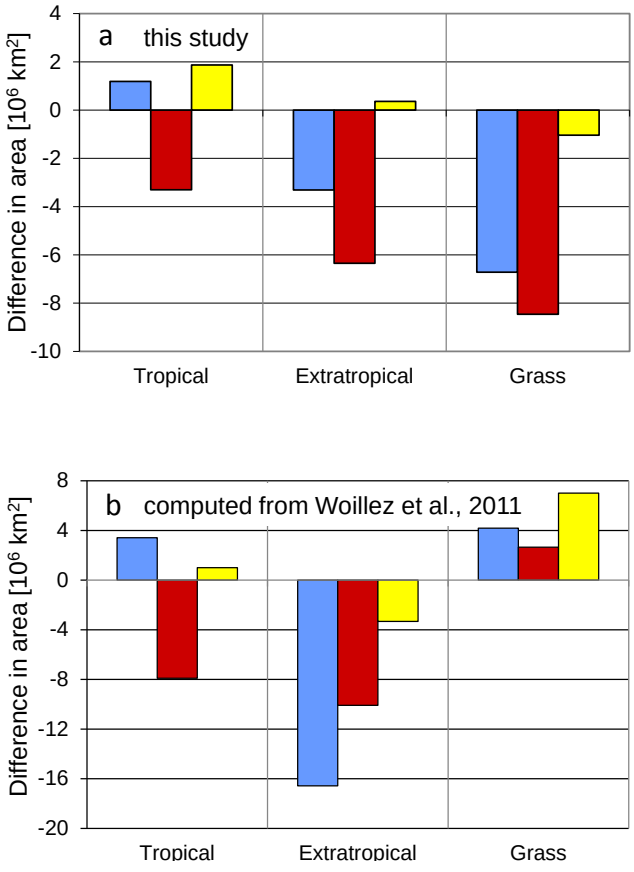

Fig. 9. Same as Fig. 6, except that in the upper part **(a)**, aggregated PFTs are depicted. Tropical: tropical woody PFT = tropical evergreen and deciduous trees and raingreen shrubs; Extratropical: extratropical woody PFT = evergreen and deciduous trees and deciduous shrubs; Grass: C3 and C4 grass. In the lower part **(b)**, factors and synergies are shown for the global foliage coverage (in 10^6 km^2) for tropical tree, combined temperate and boreal trees and grass computed from the study by Woillez et al. (2011).

and CO_2 effect lead to a reduction in grass coverage with a small negative synergy in the present study. This difference can presumably be attributed to two points. First, the strong reduction in boreal tree coverage likely provides favorable conditions for grass expansion in the simulations by Woillez et al. (2011). Second, and presumably more important, the desert area in glacial climate is by some 8×10^6 km^2 larger than in the control climate in the simulations by Woillez et al. (2011). In the present study the difference in desert area is nearly 16×10^6 km^2, i.e., almost twice as large (see Fig. 4).

4 Summary and conclusions

Differences between glacial and pre-industrial potential vegetation patterns have been attributed to differences in the climate, caused by a strong increase in ice masses and the radiative effect of lower greenhouse gas concentrations, to differences in the ecophysiological effect of lower atmospheric CO_2 concentrations, and to the synergy of the climate and the ecophysiological CO_2 factors. Most studies so far have highlighted the role of the climate and the ecophysiological effect, but little attention has been paid to the synergy, the feedback between the pure climate contribution and the pure ecophysiological contribution. For example, Woillez et al. (2011) mention that "the relative impact of glacial and CO_2 is not simply additive", but they do not quantify this impact. Therefore, the factor separation method by Stein and Alpert (1993) has been applied to this problem to explicitly quantify the climate factor f_C, the ecophysiological CO_2 factor f_E and the synergy f_{CE}. It has been shown that the synergy f_{CE} is a quantitative measure of the sensitivity of the ecophysiological CO_2 effect to climate.

The factor separation has been applied to a set of simulations with the MPI-Earth system model (MPI-ESM). The MPI-ESM in the version used in this study is able to simulate most aspects of glacial versus pre-industrial potential vegetation pattern found in reconstructions and previous simulations. This includes the reduction in fractional coverage by trees, the shift to more open vegetation and bare ground in the extratropics and subtropics, and the strong reduction in NPP. In line with previous simulations, the ecophysiological effect of CO_2 evaluated using the MPI-ESM model is stronger than the pure climate contribution for many PFTs, including tropical evergreen trees. By and large, the pure climate effect leads to a contraction or a shift in vegetation pattern and, globally, to a reduction in fractional coverage – except for raingreen shrubs which strongly benefit from the colder and drier climate. The ecophysiological effect of lower CO_2 mainly yields a reduction in fractional coverage and a strong reduction in NPP. Hence the ecophysiological CO_2 effect is the larger factor with respect to thinning of glacial forests. The synergy appears to be as strong as each of the pure contributions locally, but it is weak on global average for most plant functional types. For tropical evergreen trees, however, the synergy is globally strong and it diminishes the contraction due to the pure climate effect and due to the pure ecophysiologically available CO_2 effect by approximately by 50 per cent. In other words, without the sensitivity of the ecophysiological CO2 effect to climate, the difference between glacial and pre-industrial coverage of tropical evergreen trees between would be twice as large.

The rigorous factor separation allows for a quantitative analysis and intercomparison between models in principle. An attempt of an intercomparison with the study by Woillez et al. (2011) has been undertaken. However, such a comparison of factors evaluated from different models remains a challenge because of conceptual differences among models. A more harmonized approach is highly desirable.

Acknowledgements. The authors wish to thank Marie-Noelle Woillez for constructive comments and, particularly, for providing the data for computing the factors in synergy from their model simulations. Thanks are also due to Christian Reick for discussion, to Johanna Wolter for preparing the figures, and to two anonymous reviewers for their constructive comments.

The service charges for this publication have been covered by the Max Planck Society.

Edited by: U. Seibt

References

Berger, A.: Long-term variations of daily insolation and Quaternary climatic change, J. Atmos. Sci., 35, 2362–2367, 1978.

Bigelow, N. H., Brubaker, L. B., Edwards, M. E., Harrison, S. P. Prentice, I. C., Anderson, M., Andreev, A. A., Bartlein, P. J., Christensen, T. R., Cramer, W. , Kaplan, J. O. , Lozhkin, A. V., Matveyava, N. V., Murray, D. F., McGuire, A. D., Razzhivin, V. Y., Ritchie, J. C., Smith, B., Walker, D. A., Gajewski, K., Wolf, V., Holmquist, B. H., Igarashi, Y., Kremenetskii, K., Paus, A., Pisaric, F. J., and Volkova, V. S.: Climate change and Arctic ecosystems: 1. Vegetation changes north of 55 N between the last glacial maximum, mid-Holocene, and present, J. Geophys. Res., 108, 8170, doi:10.1029/2002JD002558, 2003.

Braconnot, P., Otto-Bliesner, B., Harrison, S., Joussaume, S., Peterchmitt, J.-Y., Abe-Ouchi, A., Crucifix, M., Driesschaert, E., Fichefet, Th., Hewitt, C. D., Kageyama, M., Kitoh, A., Laîné, A., Loutre, M.-F., Marti, O., Merkel, U., Ramstein, G., Valdes, P., Weber, S. L., Yu, Y., and Zhao, Y.: Results of PMIP2 coupled simulations of the Mid-Holocene and Last Glacial Maximum – Part 1: experiments and large-scale features, Clim. Past, 3, 261–277, doi:10.5194/cp-3-261-2007, 2007.

Brovkin, V., Raddatz, T., Reick, C., Claussen, M., and Gayler, V.: Global biogeophysical interaction between forest and climate, Geophys. Res. Lett., 36, L07405, doi:10.1029/2009GL037543, 2009.

Brovkin, V., Boysen, L., Raddatz, T., Gayler, V., Loew, A., and Claussen, M.: Evaluation of vegetation cover and land-surface albedo in MPI-ESM CMIP5 simulations, J. Adv. Model. Earth Syst., 5, 48–57, doi:10.1029/2012MS000169, 2013.

Claussen, M. and Esch, M.,: Biomes computed from simulated climatologies, Clim. Dynam., 9, 235–243, 1994.

Collatz, G. J., Ribas-Crabo, M., and Berry, J. A.: Coupled photosynthesis-stomatal conductance model for C4 plants, Aust. J. Plant Physiol., 19, 519–538, 1992.

Crowley, T. J.: Ice age terrestrial carbon changes revisited, Global Biogeochem. Cy., 9, 377–389, 1995.

Crucifix, M., Betts, R. A., and Hewitt, C. D.: Pre-industrial-potential and Last Glacial Maximum global vegetation simulated with a coupled climate-biosphere model: Diagnosis of bioclimatic relationships, Glob. Planet. Change, 45, 295–312, 2005.

Dallmeyer, A., Claussen, M., and Otto, J.: Contribution of oceanic and vegetation feedbacks to Holocene climate change in monsoonal Asia, Clim. Past, 6, 195–218, doi:10.5194/cp-6-195-2010, 2010.

Elenga, H., Peyron, O., Bonnefille, R., Jolly, D., Cheddadi, R., Guiot, J., Andrieu, V., Bottema, S., Buchet, G., De Beaulieu, J.-L., Hamilton, A. C., Maley, J., Marchant, R., Perez-Obiol, R., Reille, M., Riollet, G., Scott, L., Straka, H., Taylor, D., Van Campo, E., Vincens, A., Laarif, F., and Jonson, H.: Pollen-based biome reconstruction for southern Europe and Africa 18,000 yr bp, J. Biogeogr., 27, 621–634, 2000.

Farquhar, G. D., Caemmerer, S. V., and Berry, J. A.: A biochemical-model of photosynthetic CO2 assimilation in leaves of C3 species, Planta, 149, 78–90, 1980.

Hansen, M., DeFries, R., Townshend, J. R., Carroll, M., Dimiceli, C., and Sohlberg, R.: 2001 Percent Tree Cover, Collection 4, Vegetation Continuous Fields MOD44B,, available at: http://glcf.umiacs.umd.edu/data/vcf/, (last access: 13 July 2007), Univ. of Md., College Park, 2007.

Hantel, M. (Ed.): Observed Global Climate, Landolt-Börnstein, Group V, Geophysics, Vol. 6., Springer, Berlin Heidelberg, 2005.

Harrison, S. P. and Prentice, I. C.: Climate and CO_2 controls on global vegetation distribution at the last glacial maximum: analysis based on palaeovegetation data, biome modelling and palaeoclimate simulations, Glob. Change Biol., 9, 983–1004, 2003.

Jahn, A., Claussen, M., Ganopolski, A., and Brovkin, V.: Quantifying the effect of vegetation dynamics on the climate of the Last Glacial Maximum, Clim. Past, 1, 1–7, doi:10.5194/cp-1-1-2005, 2005.

Jungclaus, J. H., Keenlyside, N., Botzet, M., Haak, H., Luo, J. J., Latif, M., Marotzke, J., Mikolajewicz, U., and Roeckner, E.: Ocean circulation and tropical variability in the coupled model ECHAM5/MPI-OM, J. Climate, 19, 3952–3972, 2006.

Kattge, J., Knorr, W., Raddatz, T., and Wirth, C.: Quantifying photosynthetic capacity and its relationship to leaf nitrogen content for global-scale terrestrial biosphere models, Glob. Change Biol., 15, 976–991, doi:10.1111/j.1365-2486.2008.01744.x, 2009.

Kubatzki, C. and Claussen, M.: Simulation of the global biogeophysical interactions during the last glacial maximum, Clim. Dynam., 14, 461–471, 1998.

Kutzbach, J. E., Gallimore, R., Harrison, S., Behling, P., Selin, R., and Laarif, F.: Climate and biome simulations for the past 21,000 years, Quarternary Sci. Rev., 17, 473–506, 1998.

Levis, S. and Foley, J. A.: CO_2, climate-vegetation feedbacks at the Last Glacial Maximum, J. Geophys. Res., 104, 31191–31198, 1999

Marchant, R., Cleef, A., Harrison, S. P., Hooghiemstra, H., Markgraf, V., van Boxel, J., Ager, T., Almeida, L., Anderson, R., Baied, C., Behling, H., Berrio, J. C., Burbridge, R., Björck, S., Byrne, R., Bush, M., Duivenvoorden, J., Flenley, J., De Oliveira, P., van Geel, B., Graf, K., Gosling, W. D., Harbele, S., van der Hammen, T., Hansen, B., Horn, S., Kuhry, P., Ledru, M.-P., Mayle, F., Leyden, B., Lozano-García, S., Melief, A. M., Moreno, P., Moar, N. T., Prieto, A., van Reenen, G., Salgado-Labouriau, M., Schäbitz, F., Schreve-Brinkman, E. J., and Wille, M.: Pollen-based biome reconstructions for Latin America at 0, 6000 and 18 000 radiocarbon years ago, Clim. Past, 5, 725–767, doi:10.5194/cp-5-725-2009, 2009.

Mikolajewicz, U., Vizcaino, M., Jungclaus, J., and Schurgers G.: Effect of ice sheet interactions in anthropogenic climate change simulations, Geophys. Res. Lett., 34, L18706, doi:10.1029/2007GL031173, 2007.

Otto, J., Raddatz, T., and Claussen, M.: Climate variability-induced uncertainty in mid-Holocene atmosphere-ocean-vegetation feedbacks. Geophys. Rev. Lett., 36, L23710,

doi:10.1029/2009GL041457, 2009.

Otto, J., Raddatz, T., and Claussen, M.: Strength of forest-albedo feedback in mid-Holocene climate simulations, Clim. Past, 7, 1027–1039, doi:10.5194/cp-7-1027-2011, 2011.

Peltier, W.: Global glacial isostasy and the surface of the ice-age Earth: the ICE-5G (VM2) Model and GRACE, Annu. Rev. Earth Pl. Sci., 32, 111–149, 2004.

Pongratz, J., Reick, C., Raddatz, T., and Claussen, M.: A reconstruction of global agricultural areas and land cover for the last millennium, Global Biogeochem. Cy., 22, GB3018, doi:10.1029/2007GB003153, 2008.

Prentice, I. C., Jolly, D., and BIOME 6000 members: Mid-Holocene and glacial-maximum vegetation geography of the northern continents and Africa, J. Biogeogr., 27, 507–519, 2000.

Prentice, I. C., Harrison, S. P., and Bartlein, P. J.: Global vegetation and terrestrial carbon cycle changes after the last ice age, New Phytol., 189, 988–998, 2011.

Raddatz, T. J., Reick, C. H., Knorr, W., Kattge, J., Roeckner, E., Schnur, R., Schnitzler, K.-G., Wetzel, P., and Jungclaus, J.: Will the tropical land biosphere dominate the climate-carbon cycle feedback during the twenty-first century?, Clim. Dynam., 29, 565–574, 2007.

Reick, C. H., Raddatz, T., Brovkin, V., and Gayler, V.: The representation of natural and anthropogenic landcover change in MPI-ESM, J. Adv. Model. Earth Syst., doi:10.1002/jame.20022, 2013.

Roche, D. M., Dokken, T. M., Goosse, H., Renssen, H., and Weber, S. L.: Climate of the Last Glacial Maximum: sensitivity studies and model-data comparison with the LOVECLIM coupled model, Clim. Past, 3, 205–224, doi:10.5194/cp-3-205-2007, 2007.

Rohde, R., Muller, R., Jacobsen, R., Perlmutter, S., Rosenfeld, A., Wurtele, J., Curry, J., Wickhams, C., and Mosher, S.: Berkeley Earth Temperature Averaging Process, Geoinfor. Geostat.: An Overview 1 : 2, doi:10.4172/gigs.1000103, 2013

Selent, K.: Last Glacial Maximum vegetation: results from simulations with the MPI Earth System Model (MPI-ESM), Master Thesis, University Hamburg, Hamburg, 2012.

Stein, U. and Alpert, P.: Factor separation in numerical simulations, J. Atmos. Sci., 50, 2107–2115, 1993.

Stevens B., Crueger, T., Esch, M., Giorgetta, M., Mauritsen, T., Rast, S., Schmidt, H., Bader, J., Block, K., Brokopf, R., Fast, I., Kinne, S., Kornblueh, L., Lohmann, U., Pincus, R., Reichler, T., Salzmann, M., and Roeckner, E.: The Atmospheric Component of the MPI-M Earth System Model: ECHAM6, J. Adv. Model. Earth Syst., 5, 1–27, doi:10.1002/jame.20015, 2013.

Tarasov, P. E., Webb III, T., Andreev, A. A., Afanaseva, N. B., Berezina, N. A., Bezusko, L. G., Blyakharchuk, T. A., Bolikhovskaya, N. S., Cheddadi, R., Chernavskaya, M. M., Chernova, G. M., Dorofeyuk, N.I., Dirksen, V. G., Elina, G. A., Filimonova, L. V., Glebov, F. Z., Guiot, J., Gunova, V. S., Harrison, S. P., Jolly, D., Khomutova, V. I., Kvavadze, E. V., Osipova, I. M., Panova, N. K., Prentice, I. C., Saarse, L., Sevastyanov, D. V., Volkova, V. S., and Zernitskaya, V. P.: Present-day and mid-Holocene biomes reconstructed from pollen and plant macrofossil data from the former Soviet Union and Mongolia, J. Biogeogr., 25, 1029–1053, 2000.

Woillez, M.-N., Kageyama, M., Krinner, G., de Noblet-Ducoudré, N., Viovy, N., and Mancip, M.: Impact of CO_2 and climate on the Last Glacial Maximum vegetation: results from the ORCHIDEE/IPSL models, Clim. Past, 7, 557–577, doi:10.5194/cp-7-557-2011, 2011.